LA-UR-94-3388

TITLE: NONINTERCEPTIVE TRANSVERSE EMITTANCE MEASUREMENT DIAGNOSTIC FOR AN 800 MEV H^- TRANSPORT LINE

AUTHOR(S): Darryl P. Sandoval

SUBMITTED TO: Beam Instrumentation Workshop
Vancouver, B. C., Canada
October 2-6, 1994

MASTER

Los Alamos
NATIONAL LABORATORY

Form No. 836 R5
ST 2629 10/91

Noninterceptive Transverse Emittance Measurement Diagnostic For An 800 Mev H^- Transport Line*

D. P. Sandoval
Los Alamos National Laboratory
Los Alamos, NM 87545

Abstract

A nonintrusive diagnostic device that will measure the transverse-phase-space parameters of an 800 MeV H^- beam is under development. The diagnostic device will make the measurements under normal operating conditions and will not perturb the particle beam or produce unwanted radiation. The diagnostic will use the phenomenon of laser-induced photodissociation to sample the H^- beam. This paper discusses the preliminary design of the diagnostic device.

INTRODUCTION

Theoretical models and sparse experimental results show that the Los Alamos Meson Physics Facility (LAMPF) beam distribution is nonlinear in transverse phase space. It is important for transverse phase-space matching of high current beams that the Twiss parameters be understood. For example, matching into a storage ring is very critical; if the beam phase space (Twiss parameters) is understood, correction by nonlinear elements is possible. Similar considerations apply to other high intensity systems that must be understood, such as transport lines or targets.

A diagnostic device in Line D of the LAMPF for measuring the x, x' and y, y' phase space distributions would provide information which may allow improved matching into the Proton Storage Ring (PSR) as well as providing critical information for advanced projects. Ideally, one would like to have a non intrusive diagnostic which provides the users an on-line method for determining the transverse emittance of the particle beam during normal operation (at full current) without perturbing the particle beam. H^- laser neutralization techniques demonstrated on the Ground Test Accelerator (1,2) can provide such a diagnostic device. This device would obviously have the ability to provide beam profiles as well, without producing radiation (unlike the charge-collection wires currently being used elsewhere at the LAMPF).

Advances in laser technology have in the production of highly reliable high-power lasers which require minimal maintenance. This allows one to place a laser near the beamline, eliminating the need for long laser beam transport lines. The result is the ability to use a laser beam to reliably and precisely sample the H^- particle beam with little human intervention.

SYSTEM DESCRIPTION

A laser beam would be focused into a narrow cylinder with a diameter on the order of 0.2 to 0.5 mm. The laser beam will traverse the particle beam

*Work supported and funded by the US Department of Energy, Office of Defense Programs.

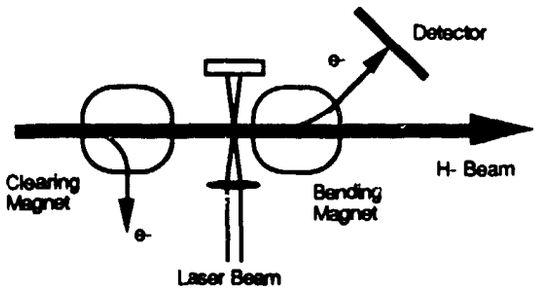

Figure 1. Schematic diagram of the transverse emittance measurement system.

neutralizing a narrow slice (x or y) of the beam. The number of photodetached electrons (and neutral particles) produced is proportional to the particle beam density and the laser energy density. One has the choice of collecting the photodetached electrons or the neutral particles to determine the x' (y') distribution. The laser beam would be scanned across the particle beam to obtain a full x, x' (y, y') distribution (into the page in Fig. 1).

Using the neutrals to measure the x' (y') distribution has the advantage that magnetic or electric fields will not effect the measurement. However, a bend and an offset beam line are required. Electron collection techniques do not require a dedicated offset beam line and can be made more compact longitudinally. Unwanted background electrons can be removed using a clearing magnet. The disadvantage is that stray magnetic and electric fields effect the trajectory of the electrons. This paper will focus on the electron collection method.

EXPECTED SIGNAL AND NOISE LEVELS

The electron signal level is calculated using the H^- beam and laser parameters given in Table 1. A baseline detector configuration is also described and evaluated.

Neutralization Fractions

The neutralization fraction f_{neut} which is defined (2) as the average probability of neutralization for beam particles that have been illuminated by the laser (Eq. 1).

$$f_{neut} = 1 - e^{-\sigma(\lambda)\phi t_i} \tag{1}$$

Where $\sigma(\lambda)$ is the photodetachment cross section for the laser wavelength λ, ϕ is the photon flux and t_i is the illumination time. The neutralization fraction assuming the following conditions was calculated using Eq. 1 with a result of f_{neut} = .99, i.e. 99% of the illuminated beam is neutralized.

Table 1. H^- beam and laser parameters.

Laser energy - 420 mJ per pulse	Neutralization cross section - 3.8 x 10^{-17} cm^2
Laser pulsewidth - 20 ns (t_i)	x rms beam width - 1.8 mm
Laser beam diameter - .3 mm	y rms beam width - 2.1 mm
Laser wavelength - 1.06 μm (Nd:YAG)	x' rms beam divergence - 0.207 mrad
Ion beam energy - 800 MeV	y' rms beam divergence - 0.189 mrad
Ion beam current - 10 mA peak current (I_p)	

Electron Signal Level Calculations

The expected signal levels (electrons at the detector) were calculated assuming the laser and ion beam parameters listed above. The available charge Q_x at the detector can be estimated by using Eq. 2. This is the signal available if this diagnostic is used as a profile monitor. The limits of integration are determined by the laser beam width and location.

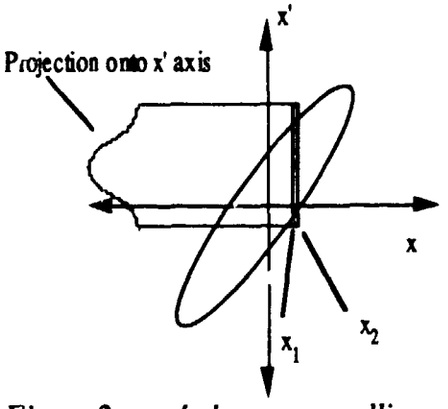

Figure 2. x, x' phase space ellipse.

$$Q_x = I_p t_i f_{neut} \int_{x_1}^{x_2} \frac{1}{\sigma_x \sqrt{2\pi}} e^{\frac{-(x)^2}{2\sigma_x^2}} dx \qquad (2)$$

Where σ_x and is the rms beam width in x, I_p is the peak current, t_i is the laser temporal pulse width and f_{neut} is the neutralization fraction. The limits of integration, x_1 and x_2, are defined by the laser beam diameter in the interaction region. Assuming a normal distribution in x' one can estimate the signal level $S_{x'1x'2}$ per x, x' pixel by using Eq. (3). See Figure 2. If one uses a width in x' of $.2\,\sigma_{x'}$ then the limits of integration are x'-.1 $\sigma_{x'}$ to x'+.1 $\sigma_{x'}$ where x' is the position of interest. This would give 20 pixels in x'. The expected signal levels are given in Table 2 for the above mentioned parameters.

$$S_{x'_1 x'_2} = C_x \int_{x'_1}^{x'_2} \frac{1}{\sigma_{x'} \sqrt{2\pi}} e^{\frac{-(x')^2}{2\sigma_{x'}^2}} dx' \qquad (3)$$

Table 2. Expected signal levels in number of electrons for various locations in x x' space. These signal levels are detectable provided they are above the noise level.

	x' location (center)	x' location (1 $\sigma_{x'}$)	x' location (2 $\sigma_{x'}$)	x' location (3 $\sigma_{x'}$)
x location (center)	8.1×10^6	5.0×10^6	1.1×10^6	9.2×10^4
x location (1 σ_x)	5.0×10^6	3.0×10^6	6.7×10^5	5.6×10^4
x location (2 σ_x)	1.1×10^6	6.9×10^5	1.5×10^5	1.2×10^4
x location (3 σ_x)	9.4×10^4	5.6×10^4	1.3×10^4	1.0×10^3

Detector Configuration and Signal Level

The baseline detector consists of an intensified camera viewing a sodium iodide scintillator (Figure 3). This detector configuration was selected as the baseline system because it uses components that we have on hand and are familiar with, not because it is the best choice.

The range (depth of penetration) of 435 keV electrons in NaI(Tl) is about 0.58 mm (3). The total path length that the electrons travel is 1.2 to 4 times the range, the ratio being largest for slow electrons in materials of high Z (3). Given the

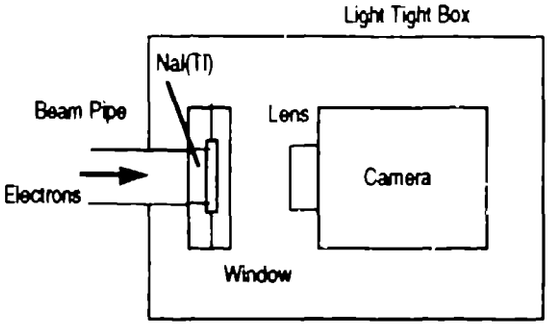

Figure 3. Schematic diagram of the baseline detector system.

above parameters, each pixel (x, x') at the detector (scintillator) will be 40 μm wide by approximately 1 cm in height. The narrow dimension is the dimension of interest (see Figure 4). In order to keep the effects caused by electron scatter in the scintillator to a minimum, the scintillator thickness will be one-half of the required resolution (approximately 20 μm).

NaI(Tl) produces about 52000 photons with a mean wavelength of 415 μm per MeV per particle if the particle is completely stopped. The energy loss across the range of the electrons is fairly linear (4). Therefore, the ratio of photons produced is equivalent to the ratio of the scintillator thickness divided by the range of the electrons. Each electron produces about 1800 photons in a 20 μm thick scintillator.

The electrons contained in the phase space pixel located at $x = 3\sigma$ and $x' = 3\sigma$ produce 780 x 10^3 photons for each 20 ns laser pulse (at the scintillator). These photons are radiated into 4π steradians and it is assumed that 10% of the photons produced will be transmitted through the lens system to detector (Camera Micro Channel Plate - MCP). A lens system magnification of one-half is also assumed. This yields an energy density of 18.7 x 10^{-12} Joules per cm^2 at the camera MCP for each laser pulse.

Background Signal Level Calculations

It is assumed that a clearing magnet can be placed upstream of the laser-ion beam interaction region to remove unwanted electrons. The rate that electrons are produced by gas stripping Γ_{bk} can be estimated (5) by using Eq. 4.

$$\Gamma_{bk} = \sigma_s \rho x \frac{I}{e} \tag{4}$$

Where σ_s (1.6 x 10^{-18} cm^2) is the stripping cross section ρ is the density of the residual gas (assumed to be 1 x 10^{-7} torr of N_2), x is the path length (assumed to be 10 cm), I is the beam current and e is the unit charge. The resulting signal to background ratio is about 1.8 x 10^8:1 or 165 dB. This assumes that the detector is gated for 250 ns.

Background due to gas stripping should not be a problem if electrons are used as the signal source. If H^0 s are used as the signal source the background due to gas stripping will be much higher due to the longer ion beam path length (x).

Noise Level Calculations

The sources of noise are background electrons, background radiation due to beam spill, photon noise and noise associated with the camera. The intensifier, the CCD array and the camera electronics will be considered as a unit. The camera being considered is an ITT intensified camera (Model F4577) which was used on GTA. Each noise source was considered separately. The results are given below.

Photon Noise

The rms noise level δ, due to the signal radiation is defined to be the square root of the variance of a Poisson distribution $\delta = \sqrt{\bar{n}}$ where $\bar{n}$ is the average number of photons incident on the detector. The rms error E_{rms} at pixel location x = 3σ and x' = 3σ is

$$E_{rms} = \frac{\bar{n}}{\delta} = \sqrt{\bar{n}} = 279. \tag{5}$$

Background Noise - Extraneous Light

Noise due to background radiation (optical) in many cases can be subtracted from the data (assuming a constant background). Great efforts will be made to eliminate any possible reflections and sources of extraneous light from the viewing area of the cameras. It is assumed that the detector will be built such that all unwanted background light is eliminated.

Background Noise - Beam Induced Radiation

The maximum expected beam spill Q_{spill} over a 1 meter length is 1 nanocouloumb per macropulse (6). Equation 6 is used to calculate the resulting radiation in Rads (6).

$$Rads = \kappa \frac{Q_{spill}}{y^2} \sin^2\theta \; e^{\frac{-\theta}{13^\circ}} \tag{6}$$

The empirical constant k = 0.15 [Rad-m^2/nC], y is the radial distance from the straight beam line to the detector and θ is the viewing angle between the spill and the detector. The optimum viewing angle is 24° with half-max at about 10° and 50°. The resulting radiation is 15.7 x 10^{-3} Rads per macropulse which is equivalent to 470 x 10^3 mips/cm^2 per macropulse[1] (mip = minimum ionizing particle) or 4.6 mips/cm^2 per μ bunch compared to 2.5 x 10^5 electrons/cm^2 per μbunch at the scintillator (at x = 3σ and x' = 3σ). This was assumed to be a worst case scenario (6). It appears that the background caused by beam spill can be neglected.

Camera Noise

The minimum detectable signal level for the intensified camera is 1 x 10^{-12} W/cm^2 at a wavelength of 400 nm. The integration time for a single frame is 16 ms. This gives a minimum detectable energy density per frame of 625 x 10^{-15} J/cm^2 compared to a signal of 18.7 x 10^{-12} J/cm^2. These numbers are for faceplate illumination.

Digitizer Noise

It is assumed that the digitizer resolution will be 2 units out of 256 or better, depending on the digitizer that is selected for the project.

---

[1] A mip is a minimum ionizing particle with 3 x 10^7 mip/cm^2 = 1 Rad.

Signal Integration

The image seen by the camera is depicted in Fig. 4. The image will be a long vertical line with its height corresponding to the particle beam width (at the point of intersection with the laser) and any spread caused by variations in particle velocity in the bend plane. The horizontal dimension contains the angular information (x') of the beam emittance for each x position which is defined by the laser).

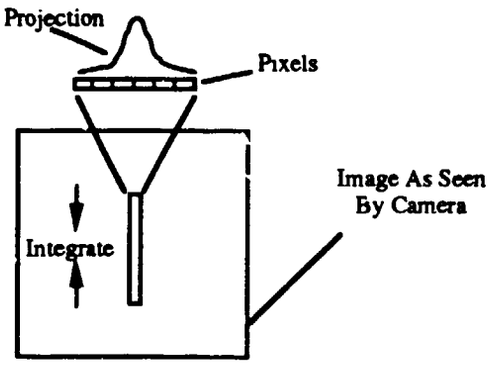

Figure 4. Illustration of a beam image as seen by the camera.

The signal will be integrated in the vertical dimension in order to remove any effects caused by variations in particle velocity. The final data set will be a 1 D array of numbers per image (per laser position).

Assuming random noise, the noise of the overall system will be decreased by a factor of $\sqrt{N}$ (N is the number of rows) when the signal is integrated. By integrating 50 lines the signal-to-noise ratio (SNR) is increased by a factor of 7.

Signal-to-Noise Ratio

The minimum detectable beam radiance is limited by the camera sensitivity and the digitizer resolution. The digitizer reduces the sensitivity of the camera by a factor of two. The sensitivity of the system becomes 1.25×10^{-12} J/cm^2. The total system SNR is approximately 15:1 at the $x = 3\sigma$, $x' = 3\sigma$ point in phase space. Integrating the signal (adding 50 video lines in the vertical dimension) increases the SNR to 106.1.

CONCLUSIONS

A viable, laser based diagnostic system can be developed that measures the transverse emittance of the LAMPF beam in Line D. Calculations show that this diagnostic system has a SNR of 106:1 when viewing a single pixel located at $x = 3\sigma$ and $x' = 3\sigma$ in transverse phase space. This implies that the emittance of better than 99.7% of the beam can be measured. The measurement phase space resolutions are x = .3 mm by x' = 41 μrad.

This paper describes a practical approach for making emittance measurements. Improvements to the detector system will increase the dynamic range and SNR. For example focusing the electron beam to a line on the scintillator will increase the irradiance (W cm^{-2}) on the camera MCP, which in turn increases the SNR. Also, using a diode array as the detector would increase the dynamic range. Several options are available and should be considered.

Effects of stray magnetic and electric fields on the electron transport must still be evaluated. The stray fields are not expected to cause complications in making the measurement. The effect of the laser beam on the electron trajectory must also be considered.

This appears to be a viable diagnostic device for measuring the transverse emittance of the LAMPF beam.

REFERENCES

1. R. C. Connolly, et. al "A Transverse Phase-Space Measurement Technique for High Brightness, H^- Beams", Nuclear Instruments and Methods in Physics Research, A312 (1992) 415-419.

2. X. W. Yuan, et. al. "Measurement of Longitudinal Phase-Space in and Accelerated H- Beam Using a Laser-Induced Neutralization Method", Nuclear Instruments and Methods in Physics Research, A329 (1993) 381-392.

3. J. B. Birks, "Theory and Practice of Scintillation Counting", Pergamon Press, Oxford, 1964.

4. Glenn F. Knoll, "Radiation Detection and Measurement, John Wiley and Sons, New York, 1989.

5. D. R. Swenson, et. al. "Non-Invasive Diagnostics for H^- Ion Beams Using Photodetachment by a Focused Laser Beam" AIP Conference Proceedings 319. Beam Instrumentation Workshop, Santa Fe, New Mexico 1993.

6. Private communication with Mike Plum. Los Alamos National Laboratory, Accelerator Operations and Technology Division.

DISCLAIMER